



INDIA METEOROLOGICAL DEPARTMENT

FORECASTING MANUAL

PART IV

COMPREHENSIVE ARTICLES ON SELECTED TOPICS

16 : MICROSEISMS AND WEATHER

BY

A. N. TANDON AND S. N. BHATTACHARYA

ISSUED BY

THE DEPUTY DIRECTOR GENERAL OF OBSERVATORIES (FORECASTING)

POONA - 5

FORECASTING MANUAL

Part IV. Comprehensive Articles on Selected Topics.

16. Microseisms and Weather

by

A.N. Tandon and S.N. Bhattacharya

1. Introduction.

1.1 What are Microseisms?

Microseisms are defined as continuous more or less regular but minute vibrations of the ground, which are not produced by earthquakes or explosions. These vibrations have periods or pseudo-periods ranging from fraction of a second to less than a few minutes and continue for a long time.

Microseismic vibrations are recorded by sensitive seismographs, which give the magnitude of the displacement at the earth's surface. The path of microseismic waves is along the surface of the earth and in that respect they resemble certain types of surface waves following earth-quakes.

The vibrations may be caused by forces due to heavy traffic or by wind on trees, buildings or high cliffs, and by some types of meteorological disturbances etc; but they differ from one another in type and period according to the cause. Regular microseisms having a range of periods between 2 to 10 seconds have long been known to be associated with large sea waves caused by various meteorological disturbances over a sea.

The major difference between microseismic records and earthquake records is that the vibrations recorded in the case of earthquakes start abruptly with displacements caused by body waves, followed by surface waves and has more or

less a definite ending. On the other hand, records of microseisms, which are in fact only surface waves have no sharp beginning; the increase or decrease of amplitude, if at all, happens rather gradually and the vibrations continue for many hours and sometimes for a few days (Fig. 1.1.1). Records of a microseismic storm and that of a near earthquake are shown in Fig. 1.1.1. and 1.1.2 respectively.

1.2 Historical background of Microseismic work

The phenomenon of microseisms was observed as early as the latter half of the nineteenth century during gravity investigations. In the year 1872 Bertelli suspending a pendulum in his basement observed its minute oscillations and associated them with minute pressure fluctuations. He observed that these oscillations were maximum in winter and minimum in summer. Rossi (1874) observed that a barometric depression was always followed by marked microseismic motion. In 1900, Father Jose Algue, S.J. had correlated the occurrence of microseisms with storms crossing the Philippine Islands.

Wiechert (1905, 1907) put forward his famous surf hypothesis to identify the cause of microseisms. According to this theory, microseisms were caused by the beating of surf on a steep coast. This hypothesis was supported by Zoepritz (1908), Benndorf (1910) and later more extensively by Gutenberg (1912, 1915, 1931).

The correlation of microseisms with hurricanes or deep low pressure areas was investigated by Zoepritz (1908), Wadati (1926) and Gherzi (1927). Gherzi (1927) and Banerji (1930) pointed out that microseisms were generated from the sea bottom under the meteorologically disturbed part of the ocean. Longuet-Higgins (1950) put forward the view that swells moving in opposite directions with the same period produce standing waves which create fluctuating pressure at the sea bottom, thereby generating microseisms.

The close correlation of microseisms having periods from 2 to 10 seconds with the presence of cyclonic storms at sea has led many workers to attempt operational use of microseisms in detecting and tracking hurricanes at sea. Kurg (1937), Ramirez (1940), Macelwane (1946) used the tripartite station method for storm tracking. Gilmore (1951, 1953) put forward the micro-ratio technique for locating the storm and assessing its intensity. Lee (1935)

found the direction of arrival of microseismic waves, from the records of the Kew Observatory, assuming that microseisms constituted mainly Rayleigh type waves. Considering that microseisms may also contain a considerable component of Love Waves, the method for finding the direction of approach of microseisms was further improved by Darbyshire (1954) using a correlation technique. Many other techniques have been employed for finding the direction of approach of microseisms such as the amplitude method (Báth 1962), Jensen's (1958, 1959, 1961) method and Teisseyre-Siemek's (1960) method. The amplitude-location method (or A-L method) for locating storm centres, has lately been used by Russian investigators (Tabulevich, 1959) and Tabulevich and Savarensky, (1962).

1.3 Seasonal variation in the amplitude of microseisms as observed at Indian Observatories

Banerji (1930) observed that microseisms of considerable amplitude are recorded on the Milne-Shaw Seismograms at Colaba during the monsoon period and also during the passage of cyclonic storms in the Indian Seas. He classified the microseisms into three types. The first type which had a period ranging from 10 to 30 sec. was recorded during the winter months when gusty wind produced waves in shallow water. The second type which was generally recorded during the months from May to September had more regular and continuous wave trains and periods ranging from 4 to 10 sec. These microseisms were generated by monsoon winds blowing over the deep sea surface. The third type had periods varying from 4 to 6 sec. and the amplitudes displayed a characteristic variation, suggesting superposition of waves of different periods. This type was recorded during the pre-monsoon and post-monsoon periods when there was a cyclonic storm in Indian Seas.

The mean amplitude (double) and period for different months at Madras recorded by Sprengnether Microseismograph during 1955 to 1959 is shown in Fig.1.3.1 (Anjaneyulu, 1961) - reproduced below. The amplitude is maximum in July and minimum in February; a second maximum occurs in November. The period has a maximum in August and minimum in January; also a second maximum and minimum may be seen in March and June respectively. The maximum amplitude and period in July and August respectively are due to monsoon type microseisms. On the other hand the maximum amplitude in November is due to greater number of storms or depressions in this month.

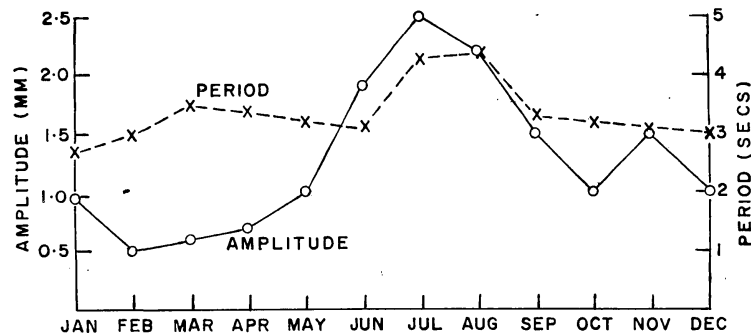


Fig. 1.3.1. Mean amplitude (double) and period for different months at Madras recorded by Sprengnether microseismograph ($T_0 = T_g = 7.5$, $V = 5000$). (Anjaneyulu, 1961)

Chakraborty and Sarkar (1958) observed that microseisms having a period of 2-3 sec. were recorded at Calcutta during the passage of Nor'Westers over the head of the Bay of Bengal. The amplitude of these microseisms at Howrah was maximum when the disturbance was over the Bay of Bengal, away from the coast and not when it was near the recording station.

2. Classification of Microseisms

2.1. Type of Microseisms

Microseisms have usually been classified according to their periods, form and duration. The types classified by Banerji (1930) have already been discussed in 1.3. Several additional types have been found in recent years and are given in Table I (mainly from Gutenberg, 1958).

Table I. Types of Microseisms

Serial No.	Period (Sec)	Type of movement	Hypothetical cause	Distance of the cause
1.	0.001-0.5	Regular	Traffic, industry, wind	Nearby
2.	0.2 - 2	Irregular	Surf, spells of heavy rain	Nearby
3.	1 - 3	Regular	Fronts, turbulent wind	Nearby
4.	1 - 4	Irregular	Effect of wind on trees and buildings	Local
5.	2 - 6	Regular	Ocean waves in extratropical disturbances	Distant
6.	4 -10	Regular	Surf driven by wind against steep coast?	Distant
7.	4 -10*	Regular	Air pressure pulsations	Medium
8.	2 -10	Regular	Monsoon and similar type of wind	Distant
9.	10-20	Regular	Water waves striking the coast	Medium
10.	20-100	Irregular	Wind? Air currents in instrumental vault?	Nearby
11.	40-100	Irregular	Freezing of ground? Icing of instruments?	Medium

Analysing the microseisms recorded at Calcutta during 1931-39 Pramanik et al (1948) classified microseisms into the following categories:

- (i) due to thunder-squalls and strong winds at Calcutta,
- (ii) due to thundersqualls and local strong winds at the head of the Bay of Bengal,
- (iii) due to southwest monsoon,
- (iv) due to land depressions and storms and
- (v) due to shallow depression, deep depression, cyclonic storm and severe cyclonic storm in the Bay of Bengal.

Microseismic investigations carried out in Australia during the IGY period (Bullen 1965) show that microseisms of periods 4-5 1/2 sec are associated with tropical cyclones, those having periods of 7-8 sec are associated with storms outside the tropics and those having ragged short-periods of 2-4 sec are associated with cold-fronts or strong easterlies. Figs. 2.1.1, 2.1.2, 2.1.3 and 2.1.4 show some typical types of microseismic records.

2.2 Microseisms and disturbed weather over sea or land

After more than half a century of observation of the microseismic phenomenon, it has now been established that microseisms having a period of 2-10

seconds are associated with sea waves caused by meteorological conditions over the ocean, such as cold fronts, high winds etc. There are, however, many fundamental points about the origin and nature of microseisms which are still not fully understood such as the "role of ocean waves, of storm position, of wind and pressure fluctuations within the storm, of water depth and of the effect of such parameters on the period and amplitude of resulting microseisms" (Ewing, Jardetsky and Press 1957).

In India, Banerji (1930) showed that microseisms were recorded at Colaba whenever the weather was disturbed over the Arabian Sea or the Bay of Bengal. Tandon (1957, 1961) observed that microseisms generated by cyclonic storms of sufficient intensity in the Bay of Bengal and also in the Arabian Sea were recorded at all inland stations of India if the storm centre was within 0-200 m depth contour. He also observed that the amplitude of microseisms was maximum at the time when the storm was crossing the coast. Fig. 2.1.1 shows simultaneous recording of microseisms at various observatories in India due to a storm in the Bay of Bengal.

The period of microseisms had been observed to be half of the period of sea water wave (Carder and Eppley, 1959). Tandon (1961) observed an increase in the period of microseisms with the increase of the intensity of the storm. It has been pointed out by Banerji (1949) that the period of microseisms increases with the distance from the source, though the increase is very small, viz., of the order of half a second for a distance of about 2000 Km. The variation is given by

$$T^2 = T_0^2 + k \Delta,$$

where T_0 is the initial period, T the recorded period at a distance Δ and $k = 1/400$.

Bukhteyev and Andreyev (1959) have correlated the observed microseismic intensity in Kurilsk Petropavlsk with the heights of sea waves near the shore. The results show that the phenomenon is correlatable, although complete correspondence is lacking. This could be attributed to the fact that microseisms are not only generated in the immediate vicinity of a coast but also under the storm centre. Tabulevich (1963) made observations of wave heights from transport ships while cruising in the middle of the Caspian Sea between latitudes 40° and 45° and noticed an increase of amplitudes of microseisms with the increase of wave heights during a storm (correlation coefficient = 0.56).

Monakhov (1959) compared the energy of microseisms (E_M) and the energy of the cyclone (E_S) using

$$K = \frac{E_M}{E_S} = \left(\frac{A}{T}\right)^2 / \frac{L^2}{S}$$

where A and T are the amplitude and period of microseisms, S is the area of water surface enclosed by the cyclone and L the total length of the isobar. He found that K varied between 0 and 5 for different regions. From this he concluded that microseisms are generated at favourable locations only.

2.3 Case Histories

All over the world microseisms have been associated with weather conditions by various workers. In India Banerji (1930), Mukherjee (1948), Tandon (1957, 1961), Nag (1959), Saha (1962), Chakraborty and Sarkar (1958) and others analysed microseisms recorded at the Indian Observatories and correlated these with meteorological conditions prevailing over the Indian seas and land areas.

A few cases are shown below (Tandon, 1957) showing the variations of period and amplitude with the position of the storm. The tracks of the three storms of November 1948, October 1949, and December 1951 used for analysis are shown in Fig. 2.3.1. Ratio of the observed microseismic amplitudes (A_o) to the normal amplitude (A_N) and the average periods for Calcutta, Hyderabad, Kodaikanal, New Delhi and Poona have been plotted in Figs. 2.3.2, 2.3.3, 2.3.4. The normal amplitude has been taken as the average microseismic amplitude on records prevailing soon before the occurrence of the storm.

Bombay Cyclone of November, 1948.

By the morning of 18 November, 1948 a depression with its central region near 11°N , 70°E was noted. It became a cyclonic storm by 1700 IST of 19th with its centre near 17°N , 66°E and moved in a northeasterly direction. It intensified into a severe cyclonic storm by 1400 IST on 20th with its centre near 18.5°N , 66.5°E . The microseismic amplitudes at the Indian Observatories began to rise only after midnight of 20th when the storm centre was near 19°N , 66.5°E . This would indicate that before this time microseisms were either not generated at all or the propagation of microseismic waves from the storm region was stopped by the intervention of some sort of a barrier. Fig. 2.3.2 shows that the maximum amplitudes were recorded at all stations when the storm crossed

the coast at 0930 IST of 22 November. After this the amplitude decreased sharply and became normal at about midnight of 22nd.

The predominant periods recorded by Wood Anderson seismograph (having a period 2 sec) at Poona were between 2 and 4 sec; a rise in periods was observed along with amplitudes. The Milne-Shaw seismographs having a period of 12 sec. gave the average periods at Hyderabad and Kodaikanal between 4 and 5 sec. At Calcutta however, the periods showed a decrease with increase of amplitude, which is rather anomalous.

Andhra Cyclone of October 1949

A shallow depression had formed on the morning of 21 October 1949 with its centre near 10°N , 95°E . It moved in a northwesterly direction intensifying gradually. At 0830 IST of 25th it lay as a cyclonic storm with its centre at 12°N , 89°E . The storm further intensified and became severe at 1730 IST of 26th with its centre at 15°N , 84.5°E . The cyclone continued to move northwest and finally crossed coast at about 0200 IST of 28th.

Fig. 2.3.3 shows the amplitudes of microseisms at various stations recorded by Milne-Shaw seismographs except at Poona where Sprengnether microseismograph was available. The amplitudes did not show any appreciable rise until the 25th morning when the depression had already become a cyclonic storm; even at this point the rise in amplitude was slow. The amplitudes started increasing rapidly from the midnight of 25th when the cyclonic storm was further intensifying. The amplitudes at all the Indian stations reached their maximum value just after the midnight of 28th while the storm was crossing the coast and then began to register a decrease. They returned to a normal value by the midnight of 29th October.

Average periods recorded during the storm at the stations ranged from 4 to 6.5 seconds. The periods show a general tendency to rise with amplitudes and show no relation to the distance from the recording station.

Bay Cyclone of December, 1951.

The weather map on 4 December 1951 showed markedly unsettled conditions south of Andaman Sea due to the presence of a trough of low pressure. By 5th evening a depression with its centre near 7.5°N , 90°E had formed. The

microseismic amplitudes at all the stations showed no increase at all. As a matter of fact the amplitudes decreased somewhat upto the midnight of 5th. The depression deepened by the 6th morning and by 6th afternoon had become a cyclonic storm, centred at 1730 IST near 10°N, 88°E. From about this time the microseismic amplitudes at all the stations began rising (Fig. 2.3.4). At 1730 IST of 8th, the storm became a severe cyclonic storm and started to move in a northeasterly direction, becoming violent on 10th morning. The amplitudes of microseisms at nearly all the stations reached maximum between the 8th morning and midnight and thereafter became somewhat steady or declined a little until the midday of 9th when they started rising again. It is significant to note here that the storm during this time was recurving and was most probably weakening in this process which may account for the diminution in microseismic amplitudes. The microseismic amplitudes reached a second maximum between 9th evening and 10th evening and then began decreasing steadily at all the stations. On 11th morning the storm was centred at 18.5°N, 89°E and showed signs of weakening. The microseismic amplitudes reached another maximum at Calcutta on 11th night, which could be attributed either to temporary increase in the intensity of the storm or due to geological factors governing the transmission of microseismic waves between the storm centre and Calcutta. Kodaikanal also showed a rise in microseismic amplitudes from 11th midnight to 12th midnight. By the morning of 13th the storm had weakened into a depression and the microseismic amplitudes at all the stations had decreased considerably and returned to their normal value by the 14th morning. The average period during the intense period of the storm for all the Indian stations comes out to be about 6.5 sec. The periods showed, in general, a rise with the amplitudes of microseisms.

3. Propagation and Nature of Microseisms

3.1 Propagation of Microseisms

Microseisms are generated when the energy of an atmospheric disturbance is transformed into the energy of ocean waves which then transmit a part of this energy either to the ocean bottom, or to a coast or both. Microseisms thus generated are transmitted as elastic waves over the surface of the earth. During transmission some perturbations occur due to differences in elastic properties and density along the path traversed by the waves. Sometimes the microseismic waves have to cut across a geological discontinuity, in which case the amplitudes may be sufficiently attenuated or the intervening discon-

tinuity may cause change in the path due to refraction. Such a discontinuity exists at the continental margins where the crustal thickness increases from 5 km to about 35 km or more and the microseismic waves are refracted unless the wave front is normal to the coast line.

The refraction of microseisms along its path was investigated by Darbyshire (1956), Darbyshire and Darbyshire (1957) and Iyer, Lambeth and Hinde (1958). From a knowledge of the bathymetric chart of the area under consideration and using the velocities appropriate for the depths, refraction diagrams could be constructed. In constructing the refraction diagrams the reciprocity principle was employed, that is, the waves were assumed to have travelled outwards from the recording station (Fig. 3.1.1).

As already stated the transmission of microseisms is often distorted by certain geological discontinuities known as microseismic barriers. At these barriers the microseisms are partially absorbed and partially reflected, and only a fraction of the total energy passes through this barrier which is of the order of noise level, unless the storm is very intense. It has been observed by Gutenberg (1929), Westernhausen (1954), Rykunov and Mishin (1961) that the transmission of microseismic waves is good if the intervening path between the source and the recording station comprises of the same tectonic unit. The attenuation of the waves is very rapid if they have to travel through different types of geological blocks. Gutenberg (1921) and Båth (1952) found that the main barrier in Scandinavia is a fault along the west coast. In the eastern part of U.S.A., a very definite barrier passing through the north of Roosevelt Roads has been found (Gilmore, 1949, 1951) (Fig. 3.1.2). Tandon (1961) observed that there are certain regions in the Bay of Bengal which attenuate transmission of microseisms; one such region appeared to be extreme northeast angle of the Bay of Bengal and the other consists of the belt of deep water just outside the 0-200 m depth contour.

The velocity of microseisms along continents and islands has been measured by various workers using tripartite station method (Sec. 5.3). Table II gives a summary of the values obtained by various workers. The values obtained by Donn and Blaik (1952) are very much lower than those obtained by other workers.

Table II - Velocity of Microseisms

Location	Velocity km/ sec	Author
St. Louis	2.7	Ramirez (1940)
Richmond, Florida	3.3	Gutenberg (1947)
Puerto Rico	4.0	„
Palomar, California	3.3	„
Guantanamo Bay, Cuba	2.6	„
Guam	3.2	Gilmore and Hubert (1948)
Cherry Point	0.6	Donn and Blaik (1952)
Miami	1.6	„
Bermuda	2.3	„

3.2 Nature of Microseisms

The nature of microseismic waves has been the subject of study by many workers ever since the early days of microseismic research. Blaik and Donn (1954) showed that microseisms showed appropriate Rayleigh wave particle motion using microseisms recorded simultaneously on three component seismographs. From their analysis of both individual cases as well as statistical treatment of a number of disturbances they concluded that microseisms are either pure Rayleigh waves or a combinations of Rayleigh waves approaching from different directions. Darbyshire (1954) concluded from the microseisms recorded at the Kew Observatory that they consist of both Rayleigh and Love waves in approximately equal proportion. Iyer (1958) observed that the ratio of Love wave to Rayleigh waves is affected by the storm intensity and its bearing. The ratio had a tendency to decrease as the storm intensified. Working with microseismic records of Rolla, Flourissant, Bloomington, Durbuque and Ann Arbar, Strobach (1965) also observed Love wave motion along with clear fundamental mode of Rayleigh waves; the proportion of Love wave was predominant in the first three stations while Rayleigh waves were dominant in the last two. In studying the microseisms due to the storm in May 1963 in the Bay of Bengal, Saha (1966) noticed that they consisted of 70% Rayleigh waves and 30% Love waves; analysing the microseisms recorded at Howrah due to storms from the same area Rykunov (1966) also noted that Love waves contributed about 25% of the total disturbance.

For rapid identification of surface waves specially designed vectorial

recorders have been used (Gutenberg and Benioff 1956, Gutenberg 1958). This instrument uses an optical method to add vectorially the vibrations of two seismographs and produce a single trace record (Fig. 3.2.1). Such records are taken on a fixed photographic plate for a particular interval (e.g. 6 mins). The combination may be made of two horizontal seismometers, or a vertical seismometer with one horizontal component or a vertical seismometer with combined vibrations of the horizontal components. In the latter combination Love wave forms a narrow loop with long axis parallel to the horizontal direction. On the other hand, for Rayleigh waves the slope of the recorded loop will be towards the vertical direction and will depend upon the relative magnification of the instrument for the particular wave. Gutenberg and Benioff (1956) during investigation of microseisms from nontropical sources found that they are mostly of the Rayleigh wave type although waves of Love type were also observed frequently.

The counterpart of microseismic waves across continents is represented by the Lg and Rg phases (channel waves) described by Ewing, Jardetzky and Press (1957 p. 219). The periods and velocity (within the limits of error) of microseisms are very similar to Lg and Rg waves. They encounter the same 'Barriers' in their propagation. Donn (1954) observed that 8-9 seconds period microseisms propagate across more than 5000 km of continent with relatively small attenuation, the particle motion being of the Rayleigh wave type. He considered these microseisms as Rg waves. Rykunov (1961) in determining the velocity of microseismic waves by correlation method found out two velocities C_1 (3.5, 3.6 km/sec) and C_2 (2.9, 3.0 km/sec) from two clear maxima of correlation coefficient between the amplitudes of pair of stations; the velocity C_2 being of the order of Rayleigh wave velocity and C_1 being that of Lg wave. The presence of Lg and Rg in microseismic propagation demonstrates that once microseisms have entered the continent they could travel large distances. This fact has been observed by various workers. Microseisms generated near Norway were propagated to Central Asia (Gutenberg, 1921). Microseisms were observed to cross North America from east to west (Gutenberg, 1951) and from Alaska to East Coast (Carder, 1955).

4. Theories of Origin of Microseisms

4.1 Wiechert, Banerji and Gherzi's work

There is no doubt, at present, that meteorological disturbances over

the sea are in some manner the cause of most of the types of microseisms observed in the 2-10 seconds period range. Many different theories have been proposed to explain the origin, nature and propagation of microseisms, but no single theory has so far been able to explain all the observed facts.

Wiechert (1905, 1907) gave the theory that microseisms are generated by the pounding of surf on a steep coast. This was vigorously supported by Gutenberg (1912, 1915, 1931). He considered that microseisms recorded over most of Europe and Asia, as far east as Irkutsk, are due to the action of surf on the steep coast of Norway. He also associated microseisms recorded in North America with the action of surf on the various coasts. Gutenberg estimated that the energy transferred from breaking surf to the coastal ground is sufficient to cause the observed microseisms. Banerji (1930) observed that microseisms are often observed simultaneously with the beginning of disturbed weather even when it is far out at sea and long before the swell reaches the shores of India. Gilmore (1951) also observed that microseisms were recorded several days before the swells from a storm could reach the coast near the recording station. According to Bradford (1935) the coasts at most points in North America are not steep but flat where most of the energy of the surf is lost due to friction of sand and rock, and thus the surf becomes weak at the time it breaks on the coast. Carder and Eppley (1959) are of the view that microseisms due to surf are confined to local coastal areas only and have periods of 1 to 2 seconds. Recent findings of Strobach (1965) however, still support that the generation of microseisms is due to some kind of coastal effect.

Banerji (1930) postulated that gravity waves on the ocean surface transfer energy to the ocean bottom. According to him, the pressure due to change in the wave heights in the region of the storm is communicated to the bottom of the ocean as a time dependent load to generate microseisms. According to this theory the sea waves and the microseismic waves should have the same periods. Banerji (1935) used a tank model and simulated fluctuations of pressure at the sea bottom due to a passing swell. He noticed such pressures are more effectively transmitted to the bottom at greater depth than in shallow depth. At intermediate depths pressure transmission is most inefficient. Scholte (1943) assuming the compressibility of water showed that the energy thus communicated to the bottom is sufficient to produce microseisms.

Gherzi (1927) postulated that microseisms are due to 'barometric pumping' resulted from fluctuating atmospheric pressures during a storm over the ocean. This idea was later supported by Bradford (1935), Macelwane (1946) and Donn (1952).

4.2 Theory of Press and Ewing

Press and Ewing (1948) extended the normal mode theory for the propagation of elastic surface waves to explain the generation and propagation of microseismic waves. They considered a homogeneous liquid layer over a homogeneous and semi-infinite solid elastic medium as a single acoustic system, giving normal mode propagation. It was noticed that the propagation of elastic waves in such a system would be dispersive; the curves of phase velocity and group velocity as a function of the ocean depth in units of wave length consisted of two branches. It was shown by Jeffreys (1925) that for a dispersive wave-train the largest amount of energy is carried by waves whose periods are near the minimum or maximum of group velocity vs period curve. Thus at a distant point, the prevailing periods observed will be those which are associated with stationary values of group velocity. Press and Ewing assuming different properties of the layers and for oceanic depth of 1500 ft. showed that the periods corresponding to the stationary group velocities are within the range of periods observed in microseisms.

4.3 Theory of Longuet-Higgins

In agreement with the findings of Miche (1944) Longuet-Higgins (1950) showed that the force F acting at the sea bottom results from the superposition of identical frequencies of opposite waves. Taking free surface, in general, as

$$\zeta = R \int_{-\infty}^{\infty} \int_{-\infty}^{\infty} A e^{i(ukx + vky + \sigma t)} dudv$$

F is given by

$$\frac{F}{\rho} = -R 4 \left(\frac{\pi}{k}\right)^2 \int_{-\infty}^{\infty} \int_{-\infty}^{\infty} A_+ A_- \sigma^2 e^{2i\sigma t} dudv \quad \dots(4.3.1)$$

where R denotes the real part, $A_+(u,v)$ and $A_-(u,v)$ are the amplitudes of oppositely directed waves, u,v are the velocities of particles along x and y axes,

$$k = \frac{2\pi}{(u^2 + v^2)\lambda}$$

λ is the wave length, σ , the angular frequency of the component waves, is a positive function of u and v and is given by

$$\sigma^2 = (u^2 + v^2)^{\frac{1}{2}} gk \tanh \left[(u^2 + v^2)^{\frac{1}{2}} kh \right],$$

h is the depth of water, ρ is its density and g the acceleration due to gravity.

From Eqn. (4.3.1) it follows that the contribution to F from any opposite pair of wave components is twice their frequency and proportional to the product of their amplitudes. The total force is the integrated sum of contributions from all opposite pairs of wave components separately. The period of observed microseisms should therefore be nearly half the period of the observed sea waves.

The phenomenon that trains of waves of the same period could meet from opposite directions can happen under several circumstances. For instance

- (i) The incident and reflected waves near a coast could interfere with each other or
- (ii) In the case of fast moving depressions where the winds veer round very quickly, trains of waves moving in opposite directions could be generated. Other situations in which such interference could take place are
- (iii) "A wind reversal because of an oncoming cold front,
- (iv) Oppositely directed winds in different parts of the ocean, whether storm conditions exist or not,
- (v) Oppositely directed swells defracted around an island and meeting on the lee side. This is applicable to any island in the Trade Wind belt" (Carder and Eppley 1959).

Longuet-Higgins theory has been supported by the work of Dinger and Fisher (1955), Tabulevich (1963) and others and is gaining increasing acceptance. One of its main results viz. that the microseismic period should be half that of the water wave period has been observed in many cases. In spite of this, the theory has not been universally accepted for various reasons. According to this theory the pressure exerted at the bottom for a given period is independent of the water depth; but in many cases it has been observed that the ocean depth plays an important factor in microseismic generation (Tandon 1961, Donn 1952). Nanda (1960) determined the force at the bottom produced by an action of suitably oriented wind with periodic rough surface as:

$$F = \text{const.} \left(\frac{1}{2hN} \right)^{\frac{1}{2}} \Omega \rho_a u_a^2 \cos \omega t \quad \dots(4.3.2)$$

where l is the length of the wave front, h is the depth of the sea, ρ_a is the density of air, u_a is the wind speed, ω is the wave frequency, Ω is the total area of the storm and $1/N$ is the fraction of latter in the phase. Although the force given in Eqn. (4.3.2) is smaller than given in Eqn. (4.3.1), it is sufficient enough to generate microseisms. The force given in Eqn. (4.3.2) is inversely proportional to the oceanic depth and therefore the generation of microseisms over the deep ocean should be less efficient as observed by many workers.

Recently in discussing the origin and properties of microseisms, Strobach (1965) postulated that the generation of microseisms results from the superposition of the outputs of a large number of seismic oscillators. These oscillators were distributed randomly both in space and time and thus the phase angles of the incoming waves were also randomly distributed. Investigating theoretically the resultant ground motion outside the generation area, the author found good agreement between his theoretical results and the particle motion diagrams of recorded microseisms.

Investigating the pressure variations produced at the ocean bottom by hurricanes using a deep (5.7 km) ocean bottom hydrophone, Latham, Anderson and Ewing (1967) observed normal microseisms with prominent spectral peaks at periods 2.8, 4.6, and 10 - sec. The maximum microseisms of periods 2.8 and 4.6 - sec occurred many hours after the peak hurricane winds have crossed the closest point to the hydrophone. On the other hand the predominant periods for wind waves and swell from the hurricane were approximately twice the periods of the 2.8 and 4.6 - sec microseismic spectral peaks respectively. Thus it seemed that the Longuet-Higgins theory of ocean wave interaction was valid, though the interaction did not take place within the storm itself. They are of the view that "the microseismic peak near 2.8 sec is produced by wind wave interaction and the microseismic peak near 5 sec is produced by swell wave interaction". The maximum amplitudes for 10 sec microseisms were observed to coincide with the time of crossing of a hurricane at the closest point to the hydrophone and these 10 sec microseisms were produced by the direct action of the same period swell on local shore lines.

5. Microseisms and Storm Tracking

5.1 Microseisms as storm detectors

The fact that microseisms in the period range 2-10 seconds are associated with cyclonic storms at sea has led many workers to make attempts at storm tracking with their aid.

Adequate information about meteorological conditions for the parts of the world where there is a vast expanse of ocean, is not always available to the forecaster. The information from swells generated by the storm reaching the coast with a speed less than 40 km per hour constitutes a rather slow process for forecasting purposes. On the other hand the generated microseismic waves could travel at the rate of about 2-3 km/sec and the presence of a storm could be detected when the storm is far out at sea. The amplitude of the recorded microseisms could also be used for assessing the intensity of the storm (Gilmore 1951).

In India, Banerji (1930) showed that the presence of microseisms on seismograph records could be used to detect the presence of depressions or storms earlier than the other forecasting methods prevalent at that time.

5.2 Lee's method

In 1935, Lee on the basis of microseisms recorded at Kew Observatory, attempted to find out the direction of approach of microseisms. He observed that the microseisms were Rayleigh waves, where ground particle moved retrogradely in ellipses in a plane containing the vertical and the direction of propagation. Thus for waves approaching from south ^{or} west, the vertical component lags by 90° behind the horizontal while for waves approaching from the north or east, vertical precedes the horizontal by 90° (Fig. 5.2.1). For microseisms travelling from northwest to southeast there will be a phase difference of 270° between the vertical and North-South components and of 90° between the vertical and East-West components. The phase differences between North-South, East-West and vertical components of microseisms recorded at the Kew Observatory were used and compared with the position of depressions over the Eastern Atlantic and Western Europe.

Following Lee, and observing that microseisms are either pure Rayleigh

waves or a combination of Rayleigh waves approaching from different directions, Blaik and Donn (1954) determined the direction of approach of waves at Palisades and Weston. Besides finding the bearing from the principle that the tangent of the angle of approach of waves would be given by the ratio of the amplitudes of the East-West and North-South components, they also found out the same by measuring the angle of the direction of elongation of the horizontal particle motion with respect to the north. The latter method was used for waves which showed a linear polarity in horizontal planes. The correct quadrant of approach of the waves was obtained from the particle motion in the East-West, North-South and vertical planes. The authors concluded that the unsatisfactory findings of the angles was due to refraction effect on the continental margin. They obtained good agreement in computing the angle of approach when the microseismic path was perpendicular to the continental margin (Donn 1954).

5.3 Tripartite method

The tripartite method for finding the direction of approach of microseisms was first applied by Kurg (1937) and Ramirez (1940). The method was tried as early as 1922 by Shaw but with no success, probably due to the fact that the elements were too far apart (about 7.5 miles). The method was given a good trial during the period of World War II by Gilmore. The principle of this method is as follows:

Three identical electromagnetic seismographs with constants suitable for recording the vibrations of the periods usually recorded in microseisms are installed so as to form a triangular array. It is preferable to make the triangle equilateral.

Let S_1 , S_2 and S_3 be the elements of the tripartite station recording an unidirectional wave as shown in Figure 5.3.1. Let A be the angle between the wave front and the line joining the stations with the first and second arrivals. Let the time differences between the first and the second arrivals be Δt_{12} and between the first and the last be Δt_{13} . Then if $S_1 S_2 = d_{12}$, $S_1 S_3 = d_{13}$ and $\angle S_2 S_1 S_3 = B$, the velocity of the wave is given by:

$$v = \frac{d_{12} \sin A}{\Delta t_{12}} \quad \dots(5.3.1)$$

also

$$v = \frac{d_{13} \sin (A + B)}{\Delta t_{13}} \quad \dots(5.3.2)$$

Therefore equations (5.3.1) and (5.3.2) give

$$\frac{d_{12} \sin A}{\Delta t_{12}} = \frac{d_{13} \sin (A + B)}{\Delta t_{13}}$$

Hence

$$\tan A = \frac{\sin B}{\frac{d_{12}}{d_{13}} \frac{\Delta t_{13}}{\Delta t_{12}} - \cos B} \quad \dots(5.3.3)$$

In practice all the three stations are connected by cables to a common recording station and the traces of vibrations from the three corresponding elements of the tripartite station are recorded on a single drum (Fig. 5.3.2). The intervals from an arbitrary time to the crest (or trough) of the same wave in each of the three traces is measured carefully. In order to achieve accuracy the drum is made to move at a fast speed (about 5 or 10 mm per second). The arrival orders are noted, and the time differences Δt_{12} and Δt_{13} are determined. The angle A may then be determined using the equation (5.3.3). Generally the average value of A from a large number of observations in well developed microseisms within an interval of 5 to 10 minutes is taken.

The optimum distance between the elements, which is generally preferred is within 600 m to 3000 m, depending mainly on the geology of the area. Smaller values of the distance between two legs make the time difference too small. On the other hand higher values make it difficult to identify the same wave on the three traces due to wave arrivals from other directions or due to Love waves which travel with a different velocity. In order to remove the latter effect the use of vertical seismographs is now-a-days preferred.

The results obtained by using the tripartite system by Gilmore (1946, 1947), Gilmore and Hubert (1948) and Donn and Blaik (1952) show that this method is capable of success under limited conditions only. Observations of microseisms in the Pacific Zone during the IGY period (Monakhov and Korchagina 1962) show only a 0 to 27% success (different for both stations and regions) in

determining the direction of approach by this method. According to Donn and Blaik (1952) and Monakhov and Korchagina (1962) the lack of success in finding the direction of approach by this method is due to the following causes:

- i) errors resulting from the measurement procedure,
- ii) superposition of microseisms approaching from different directions and
- iii) refraction of microseisms along the path of propagation.

The errors due to refraction could be eliminated by constructing refraction diagrams (Sec 3.1) for the region around the triangular array.

5.4 Micro-Ratio Technique

The diversity of results obtained in the computation of storm bearings by the tripartite method, led Gilmore (1951, 1953) to develop a new technique to detect the location and intensity of hurricanes and typhoons. The technique known as 'micro-ratio technique' depends on the fact that the ratio of amplitudes of microseisms at two recording stations, remains the same if the storm is located at a particular place, regardless of the intensity of the storm, or of the elastic properties along its path of propagation. With the help of data collected over a number of years for a large number of storms a chart for a pair of stations may be prepared by plotting at the centre of the storm the ratio of the two amplitudes of microseisms from the two recording stations and drawing lines through the points of equal ratio (Fig. 5.4.1). Thus at any time knowing the ratio of amplitudes of microseisms from two recording stations we can find out the ratio line on which the storm centre lies. Similar ratio lines could be constructed for other pairs of stations, and the position of the storm could be located on another ratio line. The intersection of the two identified ratio lines will give the position of the storm centre. In order to increase the efficiency of the method it is advisable to use ratio lines from several pairs of stations. The method presupposes that the instrumental constants at the recording stations will be maintained at the same value throughout.

For finding the intensity of the storm an amplitude chart may be used when the location of the storm is known. This is based on comparing the amplitude of the observed microseisms with the amplitudes of microseisms at the same station due to past storm of known intensity. An amplitude chart

(Fig. 5.4.2) of different intensities (eg. 70, 80, 90, 100 knots) around a station may be obtained by drawing lines through the storm centres of similar intensity (say, 90 knots) generating equal microseismic amplitude at the station. Thus at any time when the position of the storm is fixed, a comparison of the observed amplitude at the station with the amplitude charts will give the intensity of the storm.

The successful operation of these empirical methods is dependent on

- (i) the proper calibration of the seismographs and
- (ii) the assumption that the generation of microseisms takes place only from the storm and no other interfering microseisms are present.

Carder and Eppley (1959) observed that the micro-amplitude ratio from a particular place varied in some cases and this variation was reduced when an appropriate time lag was applied. It was also found that the micro-ratio depended on the intensity of the storm. They attributed the time lag to the time required by the swells to reach the generating area, or in other words the time required to create the proper conditions of microseismic generation, as required by Longuet-Higgins' theory.

5.5 Correlation method

Lee's method for determining the direction of approach of microseisms, on the assumption that the microseisms are Rayleigh waves, was not of much success. The determination of the direction was further improved by Darbyshire (1954, 1963) using a correlation method which assumes that microseisms consist of both Rayleigh and Love wave types. If θ is the angle of direction of propagation measured from northward-direction, then the eastward displacement and the northward displacement respectively are given by:

$$u_E = R(t) \sin \theta - L(t) \cos \theta$$

$$u_N = R(t) \cos \theta + L(t) \sin \theta$$

where $R(t)$ represents the Rayleigh wave motion and $L(t)$ the Love wave motion.

It was assumed that $R(t)$ and $L(t)$ were independent. The variances $\overline{u_E^2}$ and $\overline{u_N^2}$ are given by:

$$\overline{u_E^2} = \int \overline{R(t)^2} \sin^2 \theta + \int \overline{L(t)^2} \cos^2 \theta$$

$$\overline{u_N^2} = \int \overline{R(t)^2} \cos^2 \theta + \int \overline{L(t)^2} \sin^2 \theta,$$

where $\overline{R(t)}$ and $\overline{L(t)}$ are the r.m.s. values of $R(t)$ and $L(t)$.

The vertical displacement is given by

$$u_Z = k R(t - t_0)$$

where t_0 is the time lag or advance and is given by

$$t_0 = \frac{\epsilon}{2\pi} T$$

ϵ being the phase shift between the vertical displacement and the horizontal displacement of Rayleigh waves, and T , the period. In an ideal case ϵ should be 90° . Whether this difference is a lag or an advance will depend on the direction of approach.

The correlation coefficients between u_E at t and u_Z at $t + t_0$ is given by

$$r_{EZ} = \frac{\overline{R(t)} \sin \theta}{\overline{u_E}} \quad \dots(5.5.1)$$

and between u_N at t and u_Z at $t + t_0$ is given by

$$r_{NZ} = \frac{\overline{R(t)} \cos \theta}{\overline{u_N}} \quad \dots(5.5.2)$$

and between u_E at t and u_N at t is

$$\begin{aligned} r_{EN} &= \frac{[\overline{R(t)}]^2 - [\overline{L(t)}]^2}{\overline{u_E} \overline{u_N}} \sin \theta \cos \theta \\ &= \frac{1}{2} \frac{[\overline{R(t)}]^2 - [\overline{L(t)}]^2}{\overline{u_E} \overline{u_N}} \sin 2\theta \quad \dots(5.5.3) \end{aligned}$$

From (5.5.1), (5.5.2) and (5.5.3) the formula to obtain the values of θ may be written as

$$\left(\frac{r_{EN}}{r_{EZ} r_{NZ}} - 1 \right) \tan^4 \theta - \left[1 - \left(\frac{r_{EZ}}{r_{NZ}} \right)^2 \right] \tan^2 \theta - \left(\frac{r_{EN}}{r_{EZ} r_{NZ}} - 1 \right) \left(\frac{r_{EZ}}{r_{NZ}} \right)^2 = 0 \quad \dots(5.5.4)$$

The correlation coefficients were calculated using an analogue correlator.

The correct quadrant was estimated from the phase lag or advance in the three components.

Iyer (1958) observed that r_{EN} cannot be a reliable quantity in finding the direction of approach and using equations (5.5.1) and (5.5.2) he deduced

$$\tan^2 \theta = \frac{\left(\begin{matrix} -2 \\ r_{NZ} & -1 \end{matrix} \right)^{\frac{1}{2}}}{\left(\begin{matrix} -2 \\ r_{EZ} & -1 \end{matrix} \right)^{\frac{1}{2}}} \quad \dots(5.5.5)$$

During his studies of the microseisms in south Africa from horizontal components, Darbyshire (1963) extended this theory to various cases when (1) Rayleigh wave is unidirectional and Love waves from all directions, (2) no Love wave present and (3) Rayleigh wave and Love wave from the same range of directions. He found that θ is given by:

$$\tan 2\theta = \frac{2r_{EN} \bar{u}_E \bar{u}_N}{\bar{u}_N^2 - \bar{u}_E^2} \quad \dots(5.5.6)$$

which holds good in all the cases.

This method was used by Darbyshire (1954), Iyer (1958), Darbyshire and Hinde (1961) for microseisms generated from the North Atlantic depressions.

5.6 Amplitude method, Jensen's method and Teisseyre-Siemek's method

In recent years three methods namely the amplitude method (Bath 1962), Jensen's method (1958, 1959, 1961, Bath 1962) and Teisseyre-Seimek's method (1959) have been developed on the basis that microseisms contain both Love and Rayleigh type surface waves. Jensen developed his method but the theory behind it was later given by Bath (1962).

Let u_x , u_y and u_z be the displacements along the eastward, northward and vertical directions and R (R_H corresponding to horizontal and R_z corresponding to vertical) and L be the amplitudes of Rayleigh and Love waves respectively. It is assumed that both Rayleigh and Love waves have the same frequency ω . If θ be the direction of approach as measured from north through east, the eastward and northward components of R and L are given by

$$\begin{aligned} R_x &= R_H \sin\theta & , & & L_x &= -L \cos\theta ; \\ R_y &= R_H \cos\theta & , & & L_y &= L \sin\theta . \end{aligned} \quad \dots(5.6.1)$$

If γ is the phase difference between Love and horizontal Rayleigh waves, then the displacements at any time t along east, north and vertical are given by:

$$\begin{aligned} u_x &= R_x \sin \omega t + L_x \sin (\omega t + \gamma) \\ u_y &= R_y \sin \omega t + L_y \sin (\omega t + \gamma) \\ u_z &= R_z \sin \left(\omega t - \frac{\pi}{2} \right) \end{aligned} \quad \dots(5.6.2)$$

The moments of measuring the horizontal in 'amplitude method' are chosen at the instance when $u_z = 0$, whence

$$\begin{aligned} u_x &= R_x + L_x \cos\gamma \\ u_y &= R_y + L_y \cos\gamma \end{aligned} \quad \dots(5.6.3)$$

Assuming Rayleigh and Love waves are uncorrelated, the phase angle γ assumes all values between $-\pi$ and $+\pi$ and for a large number of observations

$$\sum_n \sin\gamma = \sum_n \cos\gamma = 0 \quad \dots(5.6.4)$$

Therefore at the instants of $u_z = 0$ we have finally

$$\frac{\sum_n u_x}{\sum_n u_y} = \frac{R_x}{R_y} = \tan\theta \quad \dots(5.6.5)$$

Again differentiating u_x , u_y in the equations (5.6.2) with respect to t we have

$$\begin{aligned} \frac{du_x}{dt} &= \frac{dR_x}{dt} \sin \omega t + \omega R_x \cos \omega t + \frac{dL_x}{dt} \sin (\omega t + \gamma) \\ &\quad + \left(\omega + \frac{d\gamma}{dt} \right) L_x \cos (\omega t + \gamma) \end{aligned}$$

and

$$\begin{aligned} \frac{du_y}{dt} &= \frac{dR_y}{dt} \sin \omega t + \omega R_y \cos \omega t + \frac{dL_y}{dt} \sin (\omega t + \gamma) \\ &\quad + \left(\omega + \frac{d\gamma}{dt} \right) L_y \cos (\omega t + \gamma) \end{aligned} \quad \dots(5.6.6)$$

The moments of measuring the slopes in the horizontal displacements in Jensen's method are chosen at the instants when $|U_z| = \max$ and the equation (5.6.6) gives

$$\begin{aligned} \frac{du_x}{dt} &= \omega R_x + \frac{dL_x}{dt} \sin\gamma + \left(\omega + \frac{d\gamma}{dt} \right) L_x \cos\gamma \\ \frac{du_y}{dt} &= \omega R_y + \frac{dL_y}{dt} \sin\gamma + \left(\omega + \frac{d\gamma}{dt} \right) L_y \cos\gamma \end{aligned} \quad \dots(5.6.7)$$

and thus the equations (5.6.4) and (5.6.7) give the formula for Jensen's method as

$$\frac{\sum_n \frac{du_x}{dt}}{\sum_n \frac{du_y}{dt}} = \frac{R_x}{R_y} = \tan\theta \quad \dots(5.6.8)$$

In Teisseyre-Siemek's method u_E , u_N and R_Z are measured at the instant $u_Z = 0$. Thus from the equation (5.6.3) we get

$$u_x \sin\theta + u_y \cos\theta = R_H$$

or

$$\frac{u_x \sin\theta}{R_Z} + \frac{u_y \cos\theta}{R_Z} = \frac{R_H}{R_Z} \quad \dots(5.6.9)$$

Since R_H/R_Z is constant the equation (5.6.9) represents a straight line whose normal makes an angle θ with northward axis.

Thus in the amplitude method u_x and u_y are measured at the instant when $u_z = 0$ in well developed groups and equation (5.6.5) may be used to find the direction of the source of microseisms.

On the other hand in Jensen's method, slopes of the horizontal displacements $\frac{du_x}{dt}$ and $\frac{du_y}{dt}$ are measured at the instant when u_z is maximum in well developed groups and equation (5.6.8) may be used to find the direction.

In Teisseyre-Siemek's method u_x , u_y and R_Z are measured at the instant $u_Z = 0$ in well developed wave groups. $\frac{u_y}{R_Z}$ is plotted against $\frac{u_x}{R_Z}$. The direction of approach is perpendicular to the straight line passing through these points. Here the axes u_x/R_Z and u_y/R_Z are taken as eastward and northward respectively.

These methods were applied by B ath in a few cases of microseisms recorded in Scandinavia (Fig. 5.6.1). The results agreed within the limits of error. Nag (1966) also used the first two methods for a storm in the Bay of Bengal.

It was also pointed out by B ath that the first two methods can be applied when two or more simultaneous sources of microseisms exist, provided the angular separation between the sources at the recording station is sufficiently large and the sources are of comparable strength.

5.7 Amplitude - Location method

Tabulevich and Savarensky (1962) doubted the applicability of the tripartite station method or the harmonic analysis of microseisms, since the microseisms could be due to the superposition of waves approaching from separate sources and the sources of excitation could be non-harmonic in nature. A method known as the amplitude location method or simply the A-L method has been used and discussed by some Russian authors (Tabulevich 1959, Tabulevich and

Savarensky 1962, Veshyakov 1963) for locating depressions and storms. This method follows from the principle that the intensity of vibration at a station is dependent on the distance between the source of microseisms and the recording station, the form of the wave front, and the attenuation along the path of propagation.

Here the ratio of the distances d_1 and d_2 from the source M to the first station S_1 and second station S_2 respectively (Fig. 5.7.1) is obtained as

$$k = \frac{d_1}{d_2} = \frac{A_2^{n_2}}{A_1^{n_1}}$$

where A_1, A_2 are the averaged microseismic amplitudes at the two recording stations, n_1, n_2 are coefficients depending on the form of the wave front and the nature of attenuation along the microseismic path ($1 \geq n \geq \frac{2}{3}$). Taking S_1 as the origin, $S_1 S_2$ as x - axis and $S_1 S_2 = B$, it may be shown that source $M(x, y)$ has the locus

$$\left(x - \frac{k^2}{k^2-1} B\right)^2 + y^2 = \left(\frac{k}{k^2-1} B\right)^2 \quad \dots(5.7.1)$$

which is the equation of a circle with its centre at $N(b, 0)$ where

$$b = \frac{k^2}{k^2-1} B \text{ and radius } r = \frac{k}{k^2-1} B.$$

Thus knowing the value of k from two recording stations we can find out the circle on which the source lies.

Taking records of microseisms from stations S_1, S_2, S_3 which satisfy the condition of synchronism (i.e. microseisms recorded at these stations are recorded from a single source which may be verified from the relative variations in amplitude and frequency of the stations), and taking several pairs of stations and drawing the appropriate circles a point, or an area is obtained from the intersection of the circles obtained from each pair of stations. The point or area may be regarded as the location of the source (Fig. 5.7.2).

This method was used in finding the location of depressions in the Caspian sea and the Atlantic ocean (Tabulevich and Savarensky 1962). It was assumed that $n_1 = n_2 = 1$. This assumption only broadens the area but the location remains correct.

5.8 Other methods

Hinde and Gaunt (1966) used two stations having specially built three component seismometers of constant response between 0.05 to 0.5 cps range. The

direction of approach could be obtained if a unidirectional wave arrived in a direction making an angle α with the line joining the two stations. If f is the frequency of the wave and φ the phase difference in degrees between the two stations then

$$\text{Sec } \alpha = \frac{d \times 360}{v} \times \frac{f}{\varphi}$$

where d is the distance between the stations in kilometres and v is the phase velocity. The authors assumed $v = 2.59$ km/sec following Darbyshire and Darbyshire (1957). The values of f as a function of φ was obtained from the outputs of the six seismometers, three at one station and three at the other. The recording of all the six seismometers was done centrally, and records digitised at 1 second interval. f could thus be plotted against φ and from the curves through these points f/φ could be obtained as the reciprocal of the slope of the curve. A correction in α was made for small instrumental phase lag.

Strobach (1965) described two methods for the determination of the direction of approach of microseisms. He presupposed that the generation of microseisms resulted from the superposition of the outputs of a large number of seismic oscillators. The first method was based on his findings what he termed as the 'beam pattern'. This was obtained by constructing horizontal particle motion of microseisms and measuring the length and azimuth of the major axis of each orbit which was nearly elliptical. The sums of amplitudes as a function of the azimuth were constructed to form the 'beam pattern'. Since all patterns were drawn on the same scale, the beams could be interpreted as the mean amplitude. The second method was based on the statistical finding that a very large vertical amplitude is, with a high statistical probability, associated with a large horizontal amplitude nearly in the mean direction of approach. To apply this method about 10 time intervals were chosen where the amplitudes in the vertical seismogram showed large amplitudes. At these time intervals a three dimensional particle motion was constructed by representing the orbit in the horizontal and vertical planes. The mean direction of the major axes in the horizontal orbits lay in the direction of the path of propagation of the waves. The particle motion in the vertical planes could be used to find the right quadrant.

6. Discussion

In spite of more than half a century of observations and a very large amount of published literature on microseisms, many fundamental facts about their nature, origin and propagation are still not clearly understood. There is however no doubt that meteorological disturbances over the ocean are responsible for the generation of regular microseisms in the 2-10 seconds period range. The mechanism as to how the atmospheric energy is transferred to the ocean bottom, through the depth of ocean water, still remains controversial. The theories of origin of microseisms given by Weichert and Longuet-Higgins are being generally accepted. Most observations seem to indicate that microseisms are generated under the storm area at least when the storm is far away from the coast. Surf action also prevails and adds to the generation of microseisms when the storm is approaching the coast. In many cases microseisms have been recorded soon after the formation of a cyclonic storm in the sea. The amplitudes of microseisms increase as the storm approaches the coast. It is quite possible that the mechanism of microseismic generation is different for different regions, depending upon a number of factors. In some regions more than one mechanism of generation may be operative. For example, Banerji's theory may be applicable (and Longuet-Higgins' theory in few cases) when the storm is located over the deeper parts of the ocean, whereas Longuet-Higgins' and the surf theory may be applicable when the storm is located on the continental shelf in which case there would be a good chance of the incoming and reflected swell from the coast to interfere as required in Longuet-Higgins' Theory.

Microseismic observations taken in many parts of the world have revealed that they consist of a mixture of Rayleigh and Love types of waves, the relative proportion of which varies in different regions. The ratio of Rayleigh and Love waves is also dependent on the position and intensity of the storm, as well as the geology along the path of propagation.

Microseismic records could be used for tracking storms at sea, but only under favourable circumstances. All the methods described in Sec. 5 have been applied in finding the location of the microseismic source; but all of them have achieved only limited success. The advantage of the amplitude

method and Jensen's method over the other methods is that they can give the direction of two simultaneous sources under favourable circumstances.

At present the operational use of microseisms is limited to indicate the presence of a cyclonic storm over the sea. The presence of the characteristic storm type microseisms on record may be taken as a sure indication of the presence of a storm, even if the conventional type observations are not available. In some cases the presence of a storm may be detected by microseismic observations by as much as 24 hours in advance of the other methods, but large microseismic amplitudes are usually recorded at a coastal station when the storm is within about 200 miles from the coast.

.....

REFERENCES

1. Algue, Jose. (1900: Proces-Verbaux et memoires du congres international de meteorologie, Paris, p. 131.
2. Anjaneyulu, T.S.S. 1961: Ind. Journ. Met. and Geophys., Vol.12 p. 560.
3. Banerji, S.K. 1930: Phil. Trans. Roy Soc. Lond. Vol. A 229, p. 287.
4. Banerji, S.K. 1935: Proc. Ind. Academy Sci. Vol. 1, p. 727.
5. Banerji, S.K. 1949: Assoc. Seis, Meteorol Oceanog. Phys, Scance Commune p. 30.
6. Båth, M. 1952: Geol. Foren. i Stockholm Forhandl Vol. 74, p. 427.
7. Båth, M. 1962: Geophys. Jour. R.A.S. Vol. 6, p. 450.
8. Benndorf, H. 1910: Sonderabdruck aus Geologische Rundschau, Vol. 1, p. 183 (Translation in Bull Seismo. Soc. Am. Vol. 1(1911) p. 122.
9. Bertelli, T. 1872: Bull. Met. Osserv. Collegio Rom. Vol. 9, p. 101.
10. Blaik, M. and Donn, W.L. 1954: Bull. Seismo. Soc. Am. Vol. 44, p. 597.
11. Bradford, D.C. 1935: Bull. Seismo. Soc. Am. Vol. 25, p. 323.
12. Bukhteyev, V.G. and Andreyev, T.A. 1959: Izv. AN SSSR Ser Geofiz. No.10
13. Bullen, K.E. 1965: Annals of International Geophysical Year 1957-58, Vol. 30, p. 130, Seismology, Pergamon Press.
14. Carder, D.S. 1955: Trans. Am. Geophys. Un. Vol. 36, p. 838.
15. Carder, D.S. and Eppley, R.A. 1959: The microseismic report of the US navy. A terminal report US Dept. of Commerce and Geodetic Survey.
16. Chakraborty, S.K. and Sarkar, D. 1958: Bull. Seismo. Soc. Am. Vol.48,p.181.
17. Darbyshire, J. 1954: Proc. Roy. Soc. Lond. A Vol. 223, p. 96.
18. Darbyshire, J. 1956: Mon. Not. Roy. Astron. Soc. Geophys. Suppl. Vol. 7, p. 147.
19. Darbyshire, J. and Darbyshire, M. 1957: Mon.Not.Roy. Astron. Soc. Geophys. Suppl. Vol. 7, p. 301.
20. Darbyshire, J. and Hinde, B.J. 1961: Research, Vol. 14, p. 8.
21. Darbyshire, J. 1963: Geophys. Jour. R.A.S., Vol. 8, p. 163.
22. Dinger, J.E. and Fisher, G.H. 1955: Trans. Am. Geophys. Un. Vol.36, p. 262.
23. Donn, W.L. 1952: J. Met. Vol. 9, p. 61.
24. Donn, W.L. and Blaik, M. 1952: Technical Report No. 19, Lamont Geological Observatory.
25. Donn, W.L. 1954: Trans. Am. Geophys. Un. Vol. 35, p. 821.
26. Ewing, M. and Press, F. 1952: Pontif. Acad. Sci. Scripta Varia Vol.12, p. 121.
27. Ewing, W.M. Jardetzky, W.S. and Press, F. 1957: Elastic waves in layer media, McGraw-Hill, New York.
28. Gherzi, E. 1927: Notes de seismologie Obs. de Zi-ka-wei, No.8, 1.
29. Gilmore, M.H. 1946: Bull, Seismo. Soc. Am. Vol. 36, p. 89.
30. Gilmore, M.H. 1947: Bull, Am. Met. Soc. Vol. 28, p. 73.
31. Gilmore, M.H. and Hubert, W.E. 1948: Bull. Seismo. Soc. Am. Vol.38, p.195.
32. Gilmore, M.H. 1949: Trans, Am. Geophys, Un. Vol. 30, p. 65.
33. Gilmore, M.H. 1951: U.S. Navy Annual Report-1951.
34. Gilmore, M.H. 1953: Symposium on microseisms, Sept. 1952, p.20, Nat'l Acad. Sci., Nat'l res. council.
35. Gutenberg, B. 1912: Diss. Gottingen u. Gerlands Beitr. Geophysik, Vol. 11, p. 314.
36. Gutenberg, B. 1915: Phys.Z. Vol. 16, p. 285.
37. Gutenberg, B. 1921: Veroff, Zentr. Int. Seism. Assoc. Strassburg p.1-106.
38. Gutenberg, B. 1929: Handbook der Geophysik Vol. 4, p. 264, Bortraeger, Berlin.
39. Gutenberg, B. 1931: Bull, Seismo. Soc. Am. Vol. 21, p. 1.
40. Gutenberg, B. 1947: J. Meteor. Vol. 4, p. 21.
41. Gutenberg, B. 1951: Compendium of Meteorology, p. 1303, Am. Met. Soc., Boston, Mass.
42. Gutenberg, B. and Benioff, H. 1956: An investigation on microseisms. California Inst. of Tech., Contribution No. 761.
43. Gutenberg, B. 1958: Microseisms, Advances in Geophys, Vol. 5, p. 53, Academic Press Inc., NY.
44. Hecker, O. 1906: Veröffentl geod. Inst. Potsdam (N.F.) Vol. 29.
45. Hinde, B.J. and Gaunt, D.I. 1966: Proc. Roy, Soc. Lond. A. Vol. 290, p. 297.
46. Iyer, H.M. 1958: Geophys, Jour, R.A.S. Vol. 1, p. 32.
47. Iyer, H.M., Lambeth, D. and Hinde, B.J. 1958: Nature, Vol. 181, p. 646.
48. Jeffreys, H. 1925: Mon. Not. R.A.S. Geophys, Suppl. Vol. 1, p. 288.
49. Jensen, H. 1958: Medd. Geod, Inst, Kobenhavn, Vol. 36, p. 18.
50. Jensen, H. 1959: Medd. Geod. Inst, Kobenhavn, Vol, 38, p. 23.
51. Jensen, H. 1961: Medd. Geod. Inst. Kobenhavn, Vol. 39, p. 67.
52. Kurg, H.D. 1937: Z.F. Geophysik, Vol. 13, p. 348.

53. Lee, A.W. 1935: Proc. Roy. Soc. Lond. A. Vol. 149, p. 183.
54. Letham, G.V., Anderson, R.S. and Ewing, M. 1967: J. Geophys. Res. Vol.72, p. 5693.
55. Longuet-Higgins, M.S. 1950: Phil. Trans. Roy. Soc. Lond. A. Vol. 243, p. 1.
56. Macelwane, J.B. 1946: Science Vol. 104, p. 300.
57. Miche, M. 1944: Ann. Ponte et. Chausses, Vol. 114, pp. 25, 87, 1031-164-270-292, 396-406.
58. Monakhov, F.I. 1959: Resultuti M.G.G. No.2, Izd-vo AN SSSR.
59. Monakhov, F.I. and Korchagina, O.A. 1962: Geophys. Mag. Vol. 31, p. 257.
60. Mukherjee, S.M. 1948: Ind. Met. Dept. Sci. notes Vol. 10, p. 41.
61. Nag, K.R. 1959: Jour. of Tech, Vol. 4, p. 171.
62. Nag, S.K. 1966: Ind. Journ. Met. and Geophys., Vol. 17, p. 637.
63. Nanda, J.N. 1960: J. Geophys, Res, Vol. 65, p. 1815.
64. Pramanik, S.K., Sengupta, P.K. and Chakravorty, K.C. 1948: Ind. Met. Dept., Sci. notes Vol. 10, No.120.
65. Press, F. and Ewing, M. 1948: Trans. Am. Geophys. Un. Vol. 29, p. 163.
66. Press, F. and Ewing, M. 1953: Symposium on microseisms, Sept, 1952 p.109, Nat'l Acad. Sci., Res. Council, Washington, D.C.
67. Ramirez, J.E. 1940: Bull. Seismo. Soc. Am. Vol. 30, pp. 35-84, 139-178.
68. Rykunov, L.N. and Mishin, S.K. 1961: Izv. An.SSSR,Ser Geofiz. No.6, 810.
69. Rykunov, L.N. 1961: Izv. AN.SSSR,Ser. Geofiz. No. 7, 1037.
70. Rykunov, L.N. 1966: Proc. Nat. Inst. Sc. of India. Vol. 32, p. 329.
71. Rossi, M.S. De 1874: Bull. del. Vulcanismo Italiano. I.
72. Saha, B.P. 1962: Ind. Journ. Met. and Geophys., Vol. 13, p. 81.
73. Saha, B.P. 1966: Ibid Vol. 17, p. 463.
74. Scholte, J.G. 1943: Ned. Acad. Wetenschap. Verslag, Grewone Vergader. Afdeel Natuurk. Vol. 52, p. 669.
75. Shaw, J.J. 1922: C.R. Union Geod. et. Geoph. Instt., Rome, p.52.
76. Stoneley, R. 1965: Annals Int. Geophysical Year, Vol. 30, p. 67, Seismology, Pergamon Press.
77. Strobach, K. 1965: Bull, Seismo. Soc. Am. Vol. 55, p. 365.
78. Tabulevich, V.N. 1959: Izv. AN. SSSR, Ser. Geofiz. No.11, 1694.
79. Tabulevich, V.N. and Savarensky, E.F. 1962: Studia Geophys, et. geod. Vol. 6, p. 331.
80. Tabulevich, V.N. 1963: Bull (Izv) Acad. Sci. USSR Geophys. Ser. (Eng. transl.) No. 11, p. 1006.
81. Tandon, A.N. 1961: Proceedings of Symposium on IGY Vol. 2, p. 207, Council of Sc. and Industrial Res., New Delhi.
82. Tandon, A.N. 1957: Ind. Journ. Met. and Geophys., Vol.8,p.1.
83. Teisseyre, R. and Siemek, T. 1960: Acta Geophys. Polanica Vol.8, p.312.
84. Veshyakov, N.V. 1963: Seismologicheskije Issledovanya No.5, 31.
85. Wadati, K. 1926: Geophys. Mag. Vol. 1, p. 35.
86. Westernhausen, H. 1954: Ann. Geophys. (Rome) Vol.7, p. 71.
87. Whipple, F.J.W. 1928: Z. Geophys., Vol.4, p. 417.
88. Wiechert, E. 1905: Gerlands Beitr. Geophysik Ergänzungsband Vol.2, p. 41.
89. Weichert, E. 1907: The Hague, p. 61.
90. Zoeppritz, K. 1908: Nach. Ges.Wiss. Goettingen Math. Phys. Kl. p. 2-10.

03 H GMT 02 NOV 1966

04 H

05 H

06 H

07 H

08 H

09 H

10 H

11 H

12 H

13 H

14 H

15 H

16 H

17 H

18 H

19 H

20 H

21 H

22 H

23 H

00 H GMT 03 NOV 1966

01 H

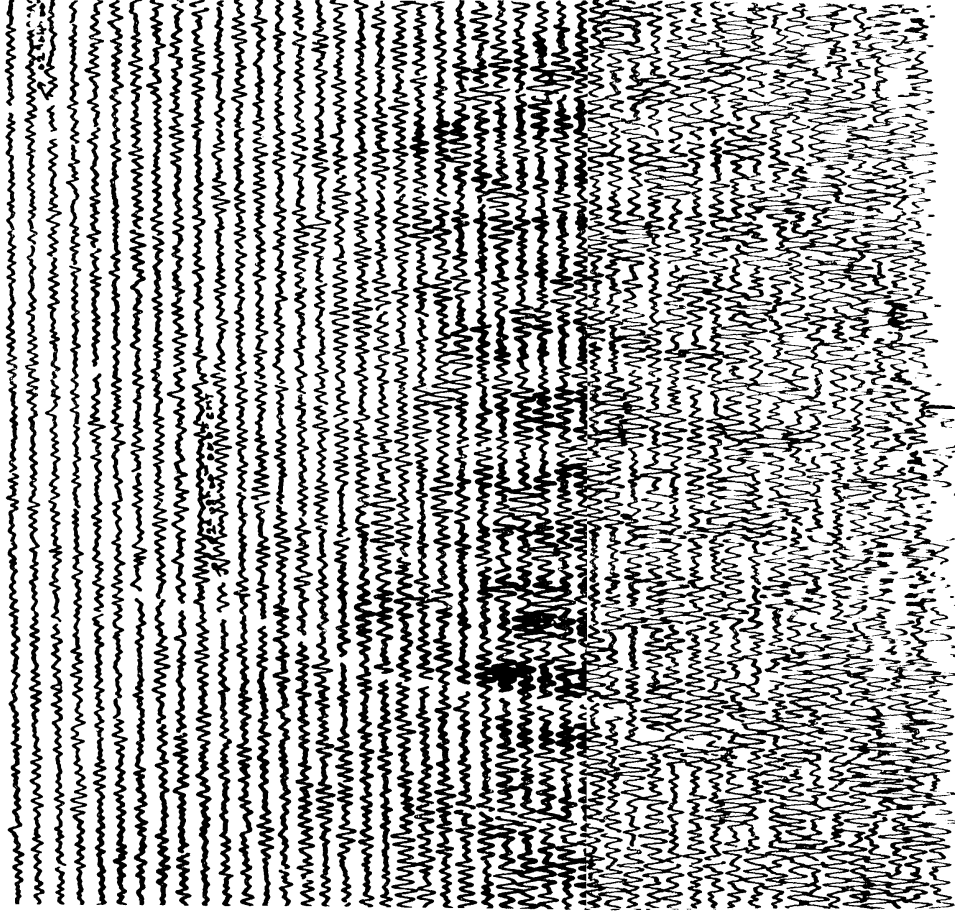


Fig.1.1.1. Microseisms recorded at the Madras observatory by a Sprengnether Horizontal Electromagnetic seismograph on - November 02, 1966 to November 03, 1966 due to a storm in the Bay of Bengal. Notice the gradual increase in amplitudes

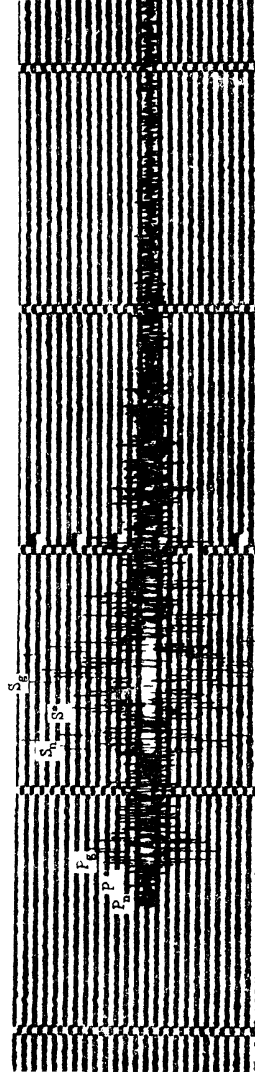


Fig.1.1.2. Seismogram of an earthquake recorded by Benioff Vertical Seismograph at Delhi. Epicentre : 29°.6 N, 81°.0 E - (Nepal-India Border), Origin time : 22 h 42 m 38.3 s, Depth of focus : 25 kms, Magnitude : 5.0

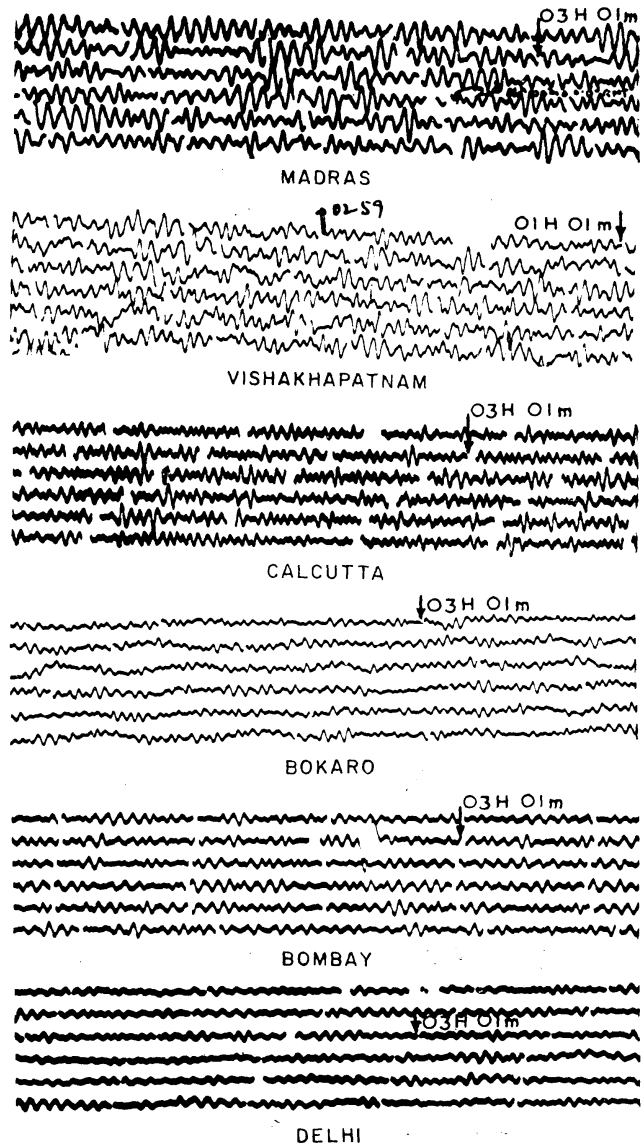


Fig. 2.1.1. Regular 3 to 6 seconds microseisms recorded simultaneously in various observatories in India on Sprengnether Electromagnetic — Seismograph due to a cyclonic storm on Nov. 21, 1966 in the Bay of Bengal

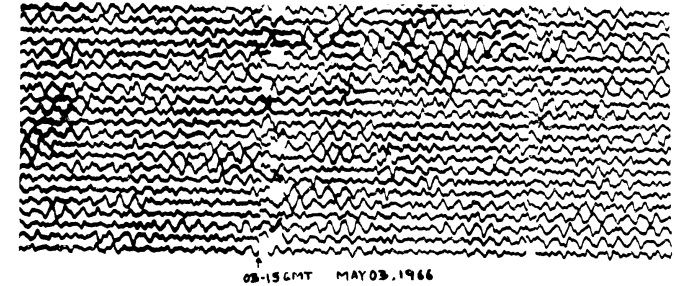


Fig. 2.1.2. Irregular microseisms of period about 2 to 3 seconds recorded at Kodaikanal on a short period vertical Benioff Seismograph

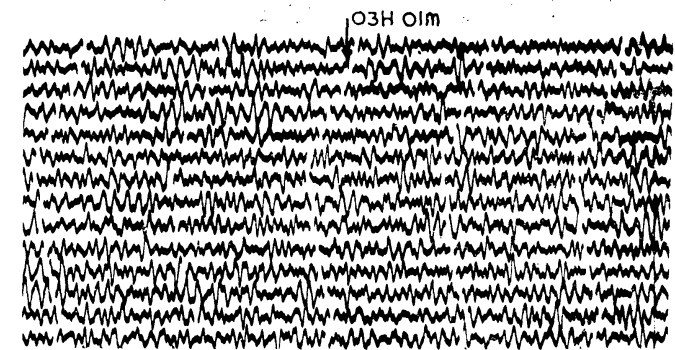


Fig. 2.1.3. Monsoon type microseisms recorded at Colaba by a — sprengnether Horizontal Electromagnetic Seismograph on July 27, 1967

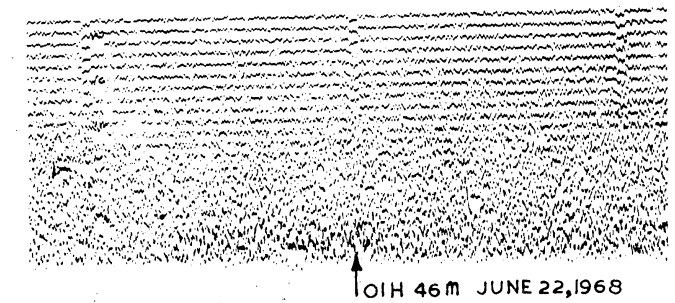


Fig. 2.1.4. Short period microseisms recorded by short period Benioff seismograph (Magnification 200 K) at Shillong during a spell of heavy incessant rain

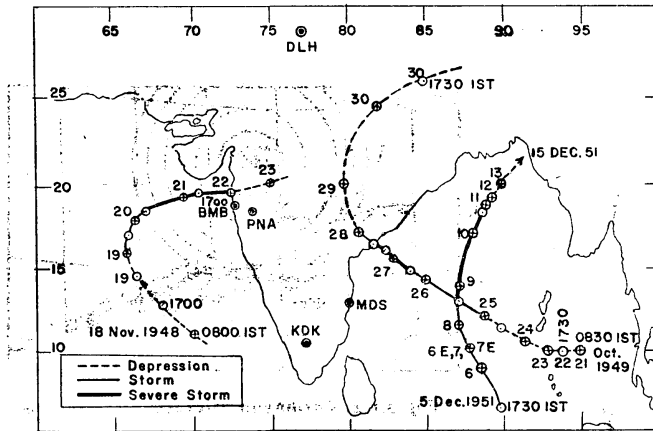
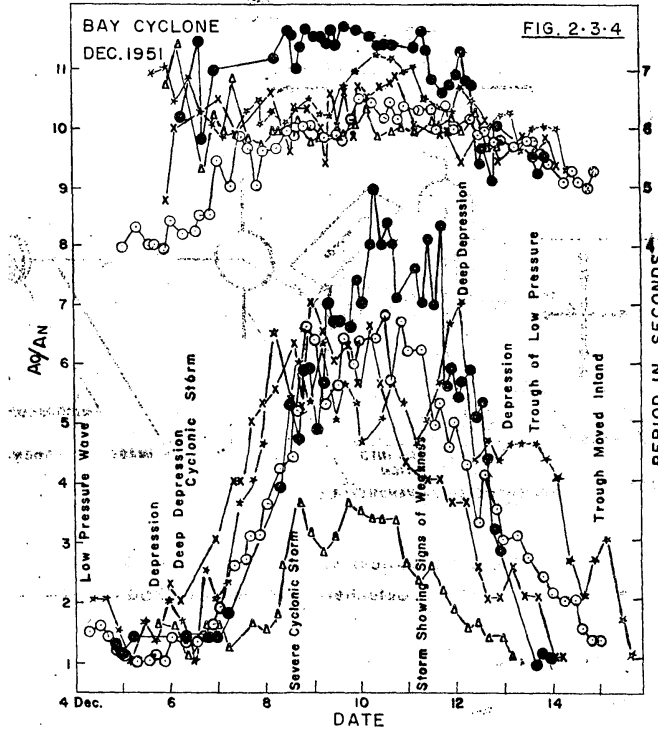
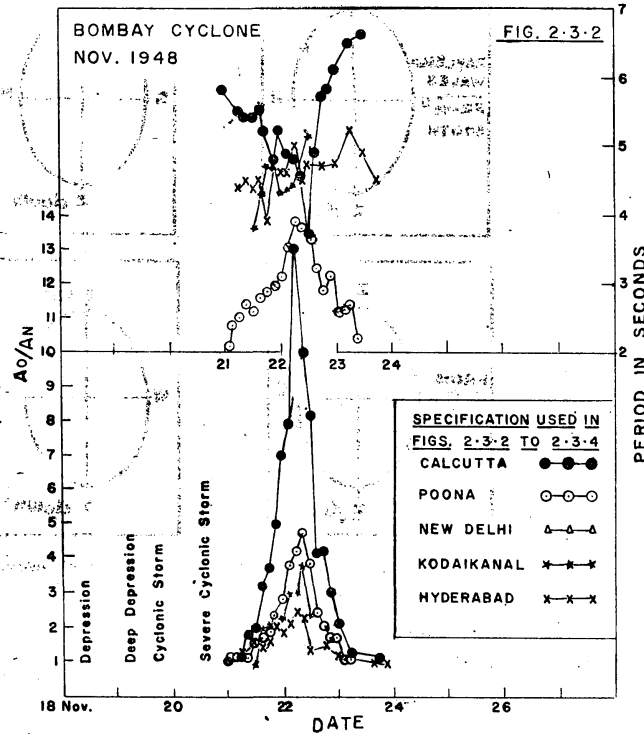
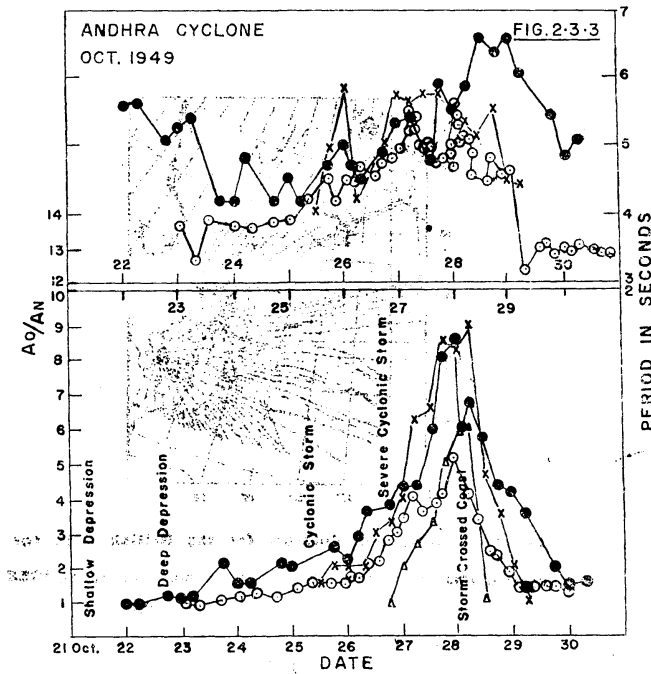


FIG. 2-3-1- TRACKS OF BOMBAY CYCLONE OF NOV. 1948, ANDHRA CYCLONE OF OCT. 1949 AND BAY CYCLONE OF DEC. 1951
(Note:- Crossed circles indicate the positions at 0800 IST or - 0830 IST and open circles at other hours, 0130, 0200, 1700, 1730 IST)

FIG. 2-3-2, 2-3-3 AND 2-3-4 :- AMPLITUDE AND PERIOD OF - MICROSEISMS DURING THE CYCLONES (TANDON, 1957)



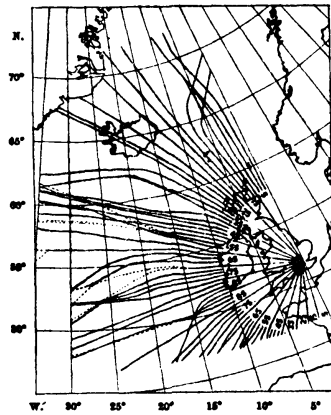


Fig. 3.1.1. Refraction diagram for the British Isles for microseisms of 6 seconds period (From Iyer et. al, 1958)

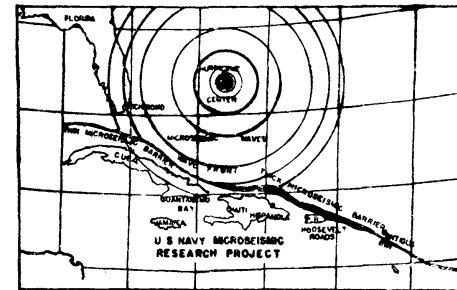


Fig. 3.1.2. Caribbean microseismic stations and the Barrier (From Gilmore, 1949)

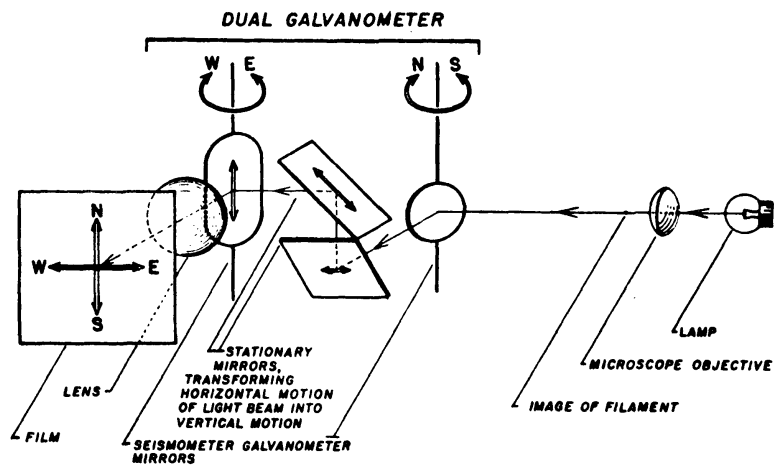


Fig. 3.2.1. Optical system of vectorial recorder (From Gutenberg and Benioff, 1956)

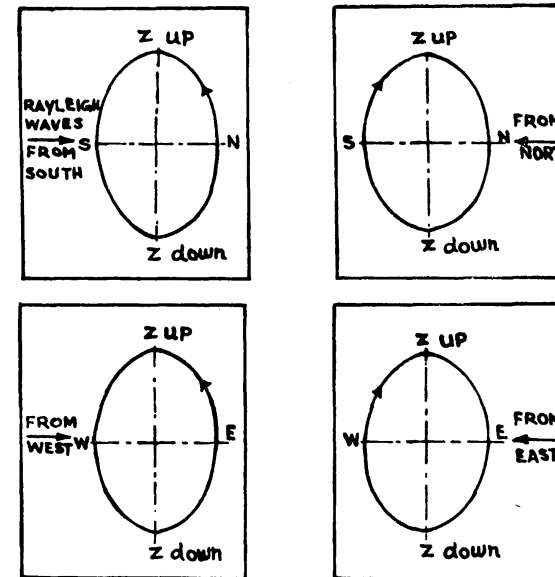


Fig. 5.2.1. Particle motion of Rayleigh wave

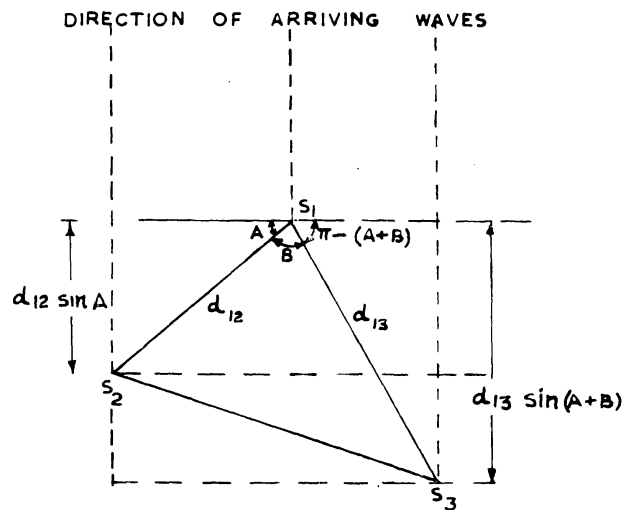


Fig. 5.3.1. Arrival of a wave front at the elements of a tripartite station

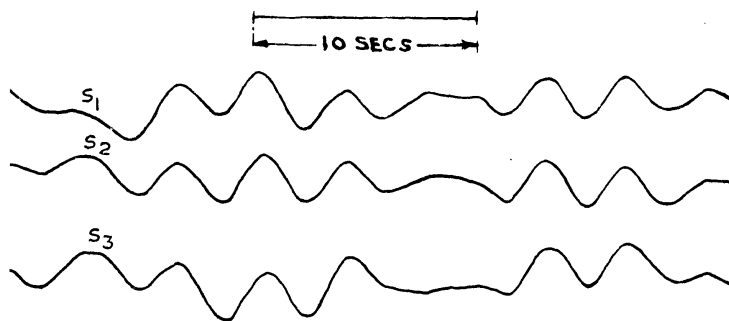


Fig. 5.3.2. Microseisms recorded by the tripartite station at Madras

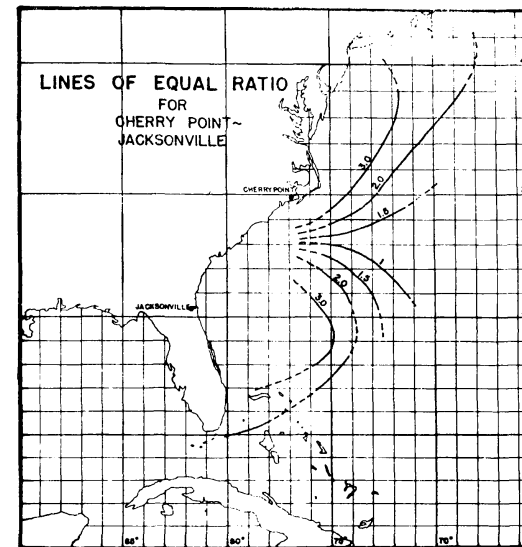


Fig. 5.4.1. Lines of equal ratio (From Gilmore, 1953)

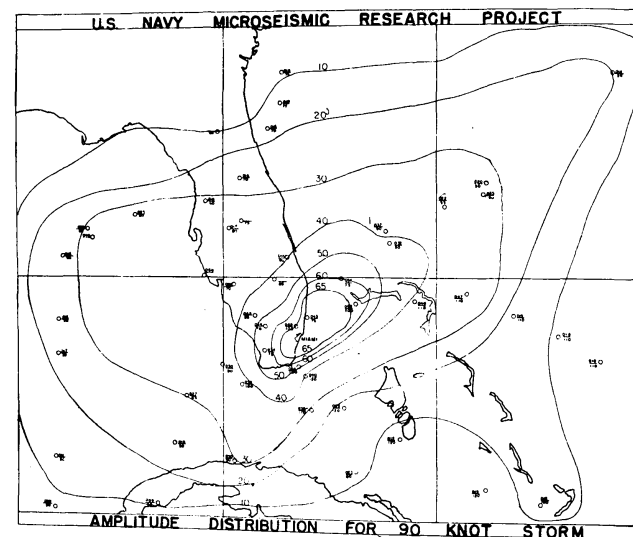


Fig. 5.4.2. Amplitude chart around Miami (From Gilmore, 1953)

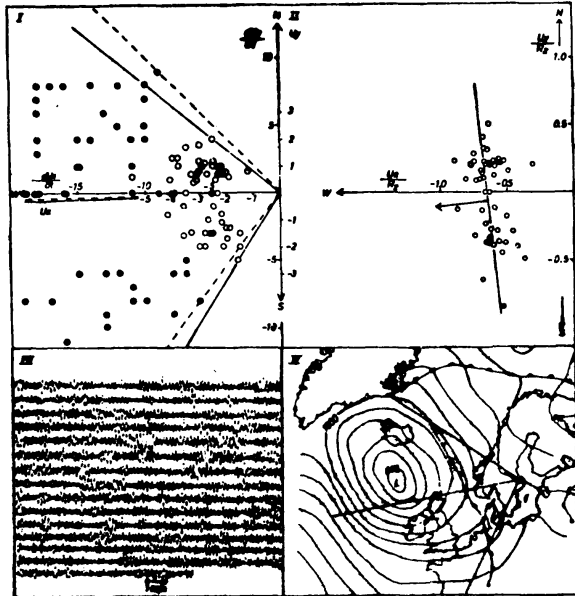


Fig. 5.6.1. Direction determinations for 1960 December 30, 00-03-09 GMT, at Uppsala:

- I. Janzen's method (dashed lines) and the amplitude method (circles and full lines).
- II. Tseluyko-Shtansk's method with its least-squares solution.
- III. Portion of the long-period vertical record at Uppsala.
- IV. Weather situation on 1960 December 30, at 00 GMT with the directions from I. included. (From Bath, 1962)

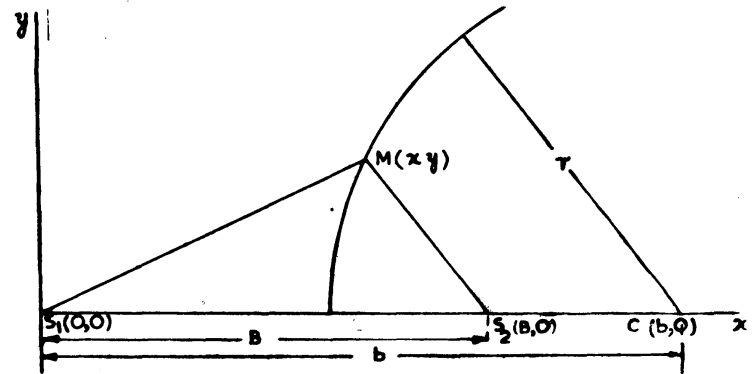


Fig. 5.7.1. Position of source of microseisms $M(x, y)$ relative to the stations S_1 and S_2

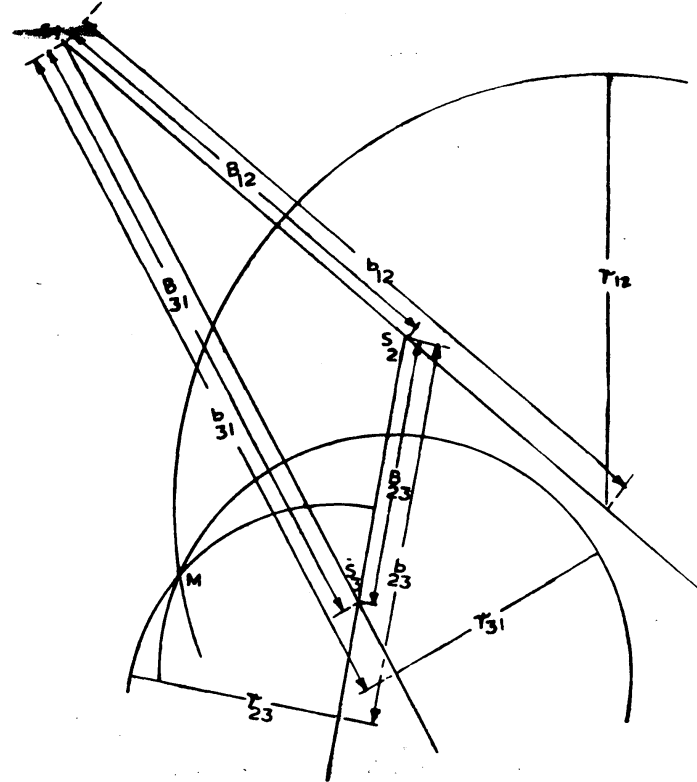


Fig. 5.7.2. Locating the microseismic source by A-L method.